Exploring Secondary Electrostatic Interactions Using Molecular Rotors: Implications for S_N2 Reactions

Binzhou Lin, [a] Hao Liu,[a] Xiaolong Huang,[a] Harrison M. Scott,[a] Perry J. Pellechia,[a] and Ken D. Shimizu*[a]

[a] Dr. B. Lin, H. Liu, X. Huang, H. M. Scott, Dr. P. J. Pellechia, Professor K. D. Shimizu
Department of Chemistry and Biochemistry
University of South Carolina
Columbia, SC 29205
E-mail: shimizu@mailbox.sc.edu

Supporting information for this article is given via a link at the end of the document.

Abstract: Benzylic and allylic electrophiles are well known to react faster in S_N2 reactions than aliphatic electrophiles, but the origins of this enhanced reactivity are still being debated. Galabov, Wu, and Allen recently proposed that electrostatic interactions in the transition state between the nucleophile and the *sp²* carbon (C2) adjacent to the electrophilic carbon (C1) transition state play a key role. To test this secondary electrostatic hypothesis, molecular rotors were designed that form similar through-space electrostatic interactions with C2 in their bond rotation transition states, without forming bonds to C1. This largely eliminates the alternative explanation of stabilizing conjugation effects between C1 and C2 in the transition state. The rotor barriers were strongly correlated with the experimentally measured S_N2 free energy. Notably, rotors where C2 was *sp²* or *sp*-hybridized had barriers that were consistently 0.5 to 2.0 kcal/mol lower than those for rotors where C2 was *sp³*-hybridized. Computational studies of atomic charges were consistent with the formation of stabilizing secondary electrostatic interactions. Further confirmation came from observing the benzylic effect in rotors where the first atom was varied, including oxygen, sulfur, nitrogen, and *sp²*-carbon. In summary, these studies provided strong experimental support for the role of secondary electrostatic interactions in the S_N2 reaction.

The S_N2 reaction is one of the most fundamental reactions in organic chemistry,[1] and accordingly has been the subject of extensive mechanistic studies.[2–6] A well-known trend is the enhanced reactivity of benzylic and allylic electrophiles.[7–16] For example, the S_N2 reactions of allyl and benzyl electrophiles are 39 and 121 times faster than structurally similar alkyl electrophiles (Figure 1a).[17,18] Previously, the enhanced reactivity of benzyl and allyl electrophiles was attributed to delocalization effects between the electrophilic carbon (C1) and the adjacent *sp²* or *sp* carbon (C2).[1,12] However, Galabov, Wu, and Allen recently proposed an alternative hypothesis based on secondary electrostatic interactions.[13] Their computational analysis found that C2 of benzyl, allyl, and alkynyl electrophiles forms more favorable electrostatic interactions in the S_N2 transition state (Figure 1b). With alkyl electrophiles, the *sp³* C2 has a slightly negative charge and forms repulsive electrostatic interactions with the negative charges of the nucleophile (Nu) and leaving group (LG). By comparison, the *sp²* C2 of benzyl electrophiles is less negative, forming weaker repulsive interactions, leading to a more stable TS and enhanced reactivity. The *sp* C2 of alkynyl electrophiles have a slightly positive charge and form attractive electrostatic interactions (not shown), leading to an even more stable TS and faster reactions.

Experimentally testing the secondary electrostatic hypothesis in S_N2 reactions is challenging due to the difficulties in differentiating it from conjugation effects. Therefore, we designed a model system where the kinetic effects of the secondary electrostatic interactions could be isolated and measured. Rather than directly mimicking the S_N2 reaction, the molecular rotors were designed to model only the through-space secondary electrostatic interactions that form in the S_N2 transition state, while avoiding confounding effects such as bond formation or conjugation at C1. Molecular rotors **1** and **2** can form

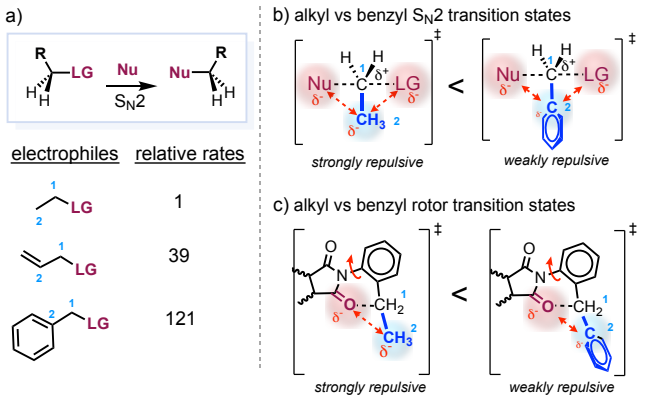

Figure 1. (a) Average relative experimental rates for the S_N2 reactions of ethyl, allyl, and benzyl electrophiles with various leaving groups (LG = I, Br, and Cl) and nucleophiles (Nu = I^-, Br^-, Cl^-, EtO^-, $S_2O_3^{2-}$, Me_3N, Et_3N, quinuclidine, pyridine, $PhNMe_2$, thiourea).[17,18] The first and second atoms (C1 and C2) are denoted with blue numbers. (b) Comparison of the secondary electrostatic interactions in S_N2 reaction transition states for benzyl and alkyl electrophiles. The length of the red double-headed arrow denotes the magnitudes of the repulsive interactions. (c) Comparison of the secondary electrostatic interactions in the molecular rotor bond rotation transition states from benzyl and alkyl R-groups.

secondary electrostatic interactions in their bond rotation TS structures (Figure 1c) similar to those in the S_N2 TS. Specifically, C2 of the *ortho*-substituent on the *N*-phenyl ring is in close-contact with the electronegative C=O oxygen. At the same time, C1 of the *ortho*- substituent does not have a leaving group and cannot form a bond, making TS stabilization via conjugation effects to C2 unlikely. Thus, if secondary electrostatic interactions influence the TS, we expect to observe their effects in the rotational barrier trends, which also provide a measure of the interactions. Conversely, if secondary interactions do not play a role, no such trends should be observed.

Another advantage of the molecular rotor model system is its sensitivity, which is essential for detecting the weak secondary electrostatic interactions. For example, the ratio of S_N2 rates for ethyl and allyl bromide (39:1), shown in Figure 1a, equates to a $\Delta\Delta G^{\ddagger}$ of only 2.2 kcal/mol.[17] Fortunately, small variations in the molecular rotor transition state energies can be observed with an accuracy of ±0.2 kcal/mol through the measurement of the rotation barriers using 2D EXSY NMR.[19,20] In addition, the magnitudes of the secondary interactions in the rotors should be similar to those in S_N2 reactions because their transition states were designed to be structurally similar. This was confirmed from a comparison of the respective TS geometries. For example, a linear correlation was observed between the O•••C2 distances in the rotors and halogen•••C2 distances in S_N2 reactions where the nucleophile and leaving group were halogens (see SI for details).[13] Additionally, the O•••C1-C2 and halogen•••C1-C2 angles exhibited similar trends.

Consequently, a series of molecular rotors **1** was designed with varying R-groups attached at the *ortho*-position that could form secondary interactions (Figure 2). The R-groups were chosen to correspond to those in S_N2 electrophiles from previous studies in which the reaction rates of various electrophiles had been experimentally measured.[17,18,21] This enabled direct comparisons between the rotor system and established SN2 rate data. The first carbon (C1) of the R-groups was a CH_2, which was kept constant across the series. The second carbon (C2) varied in hybridization (sp^3, sp^2, or *sp*) and in the number and types of attached atoms. The rotors were named according to the structure of their R-groups, which are indicated in parentheses after the compound number, such as **1**(CH_2CH_3) and **1**(CH_2Ph). Thus, rotors **1**(CH_2CH_3) and **1**($CH_2CH_2CH_3$) were designed to measure the kinetic effects of alkyl electrophiles. Rotors **1**($CH_2CH{=}CH_2$) and **1**(CH_2Ph) assessed the kinetic effects of allylic and benzylic electrophiles, and rotor **1**(CH_2CN) measured the kinetic effects of an electrophile with an *sp* C2.

Another advantage of using rotors in the ability to investigate the secondary interactions in a wider range of environments using rotors **2**. In S_N2 reactions, the first atom of the electrophile is always an sp^3 carbon, as it is involved in the key bond forming and breaking processes. Since the rotor TS does not involve bond formation to the first atom, the elemental composition and hybridization of the first atom in rotors **2** could be varied (O, S, NCH_3, C=O, $CHCH_3$).The second atom was varied between a methyl (sp^3 carbon) and a phenyl (sp^2 carbon) group. Observing the faster rotation of the secondary sp² rotors would further support and quantify the secondary electrostatic kinetic effects.

Rotors **1** and **2** were efficiently synthesized via condensation reactions of *cis*-5-norbornene-*endo*-2,3-dicarboxylic anhydride with the appropriate *ortho*-substituted aniline.[22–24] Measurement of the rate of bond rotation by dynamic NMR was facilitated by the formation of diastereomeric *syn*- and *anti*-rotamers arising from the restricted rotation of the $C_{(phenyl)}$-$N_{(imide)}$ single bond. The rotational barriers for the rotors were measured by 2D EXSY NMR in TCE-d_2, typically by following the distinct peaks for the *syn*- and *anti*-conformers of the norbornene alkene protons below the coalescence temperatures (>140 to -20 °C).

The ability of the rotors to measure the secondary electrostatic TS effects was first assessed by analysis of the measured rotational barriers ($\Delta G^{\ddagger}_{exp}$) for rotors **1**. The observed trends aligned with the expected influence of the secondary electrostatic effect. The alkyl rotors **1**(CH_2CH_3) and **1**($CH_2CH_2CH_3$) with sp^3 C2 carbons had the highest rotational barriers (22.0 and 21.7 kcal/mol). Whereas, the benzyl, allyl, and nitrile rotors, **1**(CH_2Ph), **1**($CH_2CH{=}CH_2$), and **1**(CH_2CN), with sp^2 and *sp* hybridized C2 carbons had lower barriers (21.2, 20.9, and 20.5 kcal/mol).

Not only do the rotational barrier trends match the expected secondary electrostatic interaction trends, but they also

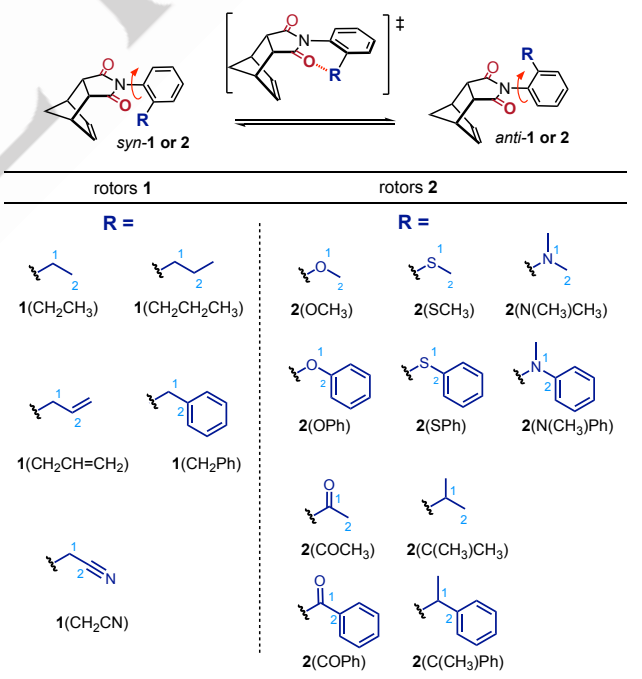

Figure 2. (top) The *syn-anti* conformational equilibrium arising from the rotation of the N-phenyl group in rotors **1** and **2**. The rotors were designed to form secondary electrostatic interactions between the *ortho*-substituents (R-groups) and the C=O oxygen, mimicking similar interactions of electrophiles in the S_N2 reaction. (bottom) Structures and names of the molecular rotors **1** and **2**. The first and second atoms of the R-groups are noted in blue numbers. In rotors **1**, the first atom is an sp^3 methylene. In rotors **2**, the first atoms are oxygen, sulfur, nitrogen, sp^2 carbon, or sp^3 tertiary carbon.

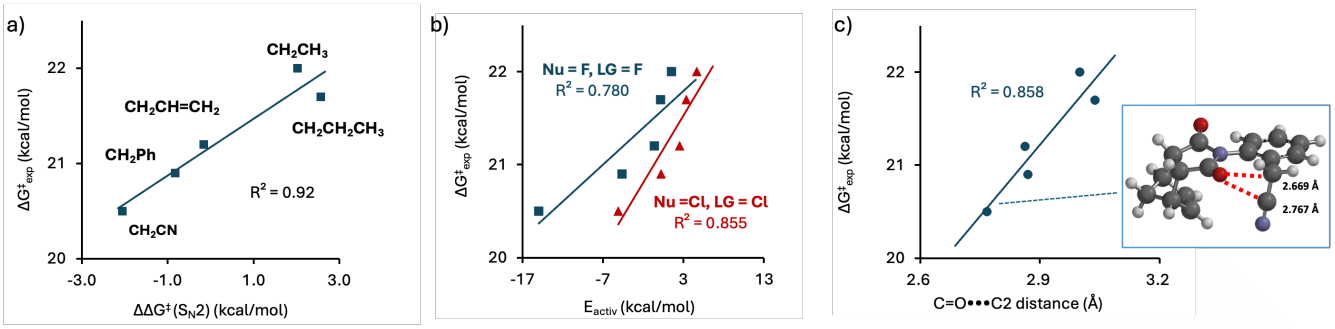

Figure 3. (a) Correlation between the NMR-measured rotational barriers ($\Delta G^{\ddagger}_{exp}$) for rotors **1** and the experimentally measured Gibbs free energies ($\Delta\Delta G^{\ddagger}_{(SN2)}$, 298 K) for the S_N2 reaction of electrophiles with the same R-groups as the rotors.[17,18,21] (b) The correlations between the experimental rotational barriers $\Delta G^{\ddagger}_{exp}$ for rotors **1** and the theoretical net activation energies of the S_N2 reactions E_{activ} from the literature.[13] (blue squares: Nu = F, LG = F; red triangles: Nu = Cl, LG = Cl) (c) The correlation between experimental rotational barriers and C=O••• C2 distances. (inset: a representative TS structure for rotor **1**(CH_2CN))

quantitatively match the experimental rate trends for S_N2 reactions. The barriers for rotors **1** ($\Delta G^{\ddagger}_{exp}$) were compared with the experimentally measured S_N2 reaction $\Delta\Delta G^{\ddagger}_{(SN2)}$ for electrophiles with the same R-groups (Figure 3a).[17,18,21] The experimental S_N2 data was originally compiled by Streitwieser and were reanalyzed by Rablen. These are an average of S_N2 reaction rates with various electrophiles (I^-, Br^-, Cl^-, EtO^-, $S_2O_3^{2-}$, Me_3N, Et_3N, quinuclidine, pyridine, $PhNMe_2$, thiourea) and leaving groups (LG = I, Br, Cl). An excellent correlation was observed (R^2 = 0.92) between the rotor and experimental S_N2 barriers across the range of R-groups that varied in the hybridization of C2 (*sp*^{3}, *sp*^{2}, and *sp*). The rotor **1** rotational barriers were also strongly correlated with the computational activation energies (E_{activ}) of S_N2 reactions, which were reported in the same study that originally formulated the secondary electrostatic hypothesis (Figure 3b).[13] For example, the plot of the experimentally measured rotational barriers for rotors **1** shows good linear correlations with the calculated energies for the S_N2 reactions of R-LG with the same R-groups as the rotors. These correlations were observed for S_N2 reactions under two different conditions where the Nu = LG = F (R^2 = 0.78) and Nu = LG = Cl (R^2 = 0.86). The correlations between the rotor **1** rotational barriers and the measured and calculated S_N2 barriers support the secondary electrostatic hypothesis. While variations in S_N2 reaction rates could arise from either secondary electrostatic or delocalization effects, this is unlikely for the rotor barriers. Since the rotors do not form bonds to C1, significant TS delocalization effects between C1 and C2 are largely ruled out. This leaves the through-space interactions of C2 as the most likely explanation for the strong correlation between the rotor and S_N2 reaction barriers.

Computational analysis of the bond rotation transition state structures provided evidence for the presence of secondary electrostatic interactions in the rotors. The rotational barriers were derived from the difference between the GS and TS energies (see SI). Despite being conducted at a modest level of theory (B3LYP-D3-6311G*), the computed rotational barriers closely matched the experimental rotational barriers with an error of just 1.1 kcal/mol.[22–24] This accuracy in the computed energies also supports the reliability of the calculated GS and TS structures.

The short intramolecular distances in the calculated TS structures were the first indications of the presence of stabilizing through-space secondary interactions. An example is shown in the inset for Figure 3c of the TS structure of rotor **1**(CH_2CN) and more are provided in the SI. The electronegative imide oxygen forms close-contacts with both the CH_2 group of C1 and the *sp*-hybridized CN group of C2. Across all rotors, C=O•••C1 and C=O•••C2 distances were consistently shorter than the sum of the van der Waal radii of the interacting oxygen and carbon atoms (3.22 Å). For example, the C1 interaction distances ranged from 2.669 to 2.738 Å, and C2 interaction distances ranged from 2.767 to 3.038 Å. The short distances for the C1 atoms can be attributed to conformational constraints imposed by the rigid *N*-phenylsuccinimide framework, which holds the C=O and CH_2 groups in close proximity. However, the short C=O•••C2 distances are more difficult to explain, as the greater conformational flexibility of the C2 group should allow it to move farther away from the C=O oxygen. Despite this flexibility, the TS structures favor short C=O•••C2 interactions, which is indicative of attractive intramolecular interactions. Quantitative support for this hypothesis came from the correlation between the secondary interaction distances and the experimental rotational barriers (Figure 3c). Rotors **1**, which had the lowest rotational barriers, also had the shortest C=O•••C2 distances, suggesting that the rotors with lower barriers form stronger interactions involving the C2 carbon.

The possibility that the lower rotational barriers of rotors with *sp*^{2}- and *sp*-hybridized C2 carbons were due to steric effects was also investigated but ruled out. The *B*-value steric parameter, derived from the rotational barriers of similar biaryl rotors, was chosen to assess the steric size of the R-groups.[25] If steric effects were responsible for the observed variations in rotational barriers, the *B*-values should directly correlate with the measured barriers. However, a plot of the *B*-values against the measured rotational barriers revealed an inverse correlation (Figure 4a), where the rotational barrier increased as the steric size of the R-group decreased. This trend is contrary to what would be expected if steric effects were driving the variations in the rotational barriers.

To confirm that the interactions of the C2 carbons in the bond rotation TS were forming attractive electrostatic interactions, their atomic charges were calculated. Among the various

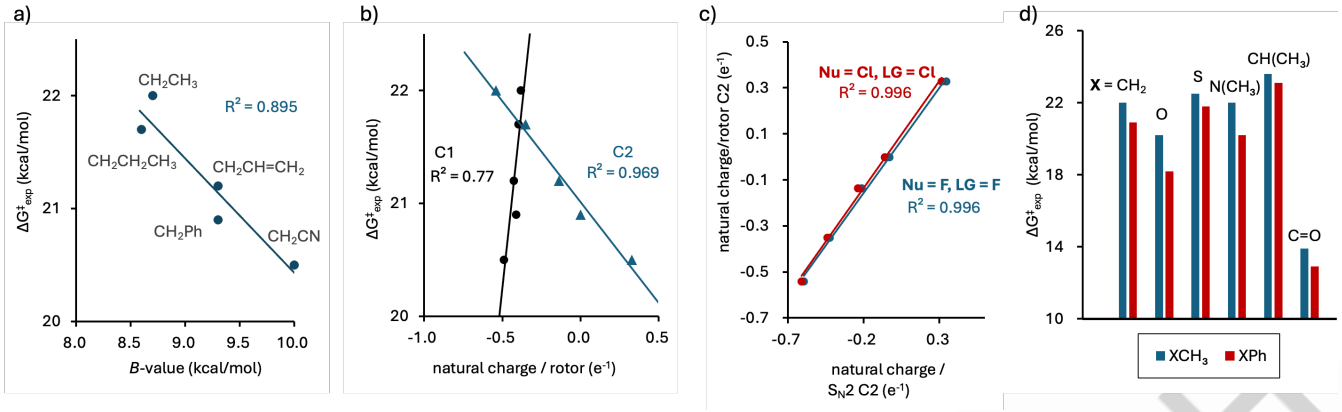

Figure 4. (a) The negative correlation between the experimental rotational barriers ($\Delta G^{\ddagger}_{exp}$) for rotors **1** and the steric parameter *B*-value for their R-groups. (b) The correlations between $\Delta G^{\ddagger}_{exp}$ for rotors **1** and the calculated natural charges on C1 and C2 of the R-groups. (c) The correlations between the calculated natural charges on C2 of the rotors **1** R-groups and the secondary carbons of structurally similar electrophiles in the S_N2 reaction from the literature.[13] (d) The comparison of the rotational barriers for rotors **1** (primary atom X = CH_2) and **2** (primary atom X = $CH(CH_3)$, O, S, NCH_3, $CH(CH_3)$, C=O) with sp^3 methyl secondary carbons (blue bars) and sp^2 phenyl secondary carbons (red bars)

methods for calculating atomic charges, natural charges were selected, as this method was used by Galabov, Wu, and Allen in their computational analysis of the S_N2 electrophiles.[13] The natural charges of the C2 carbons in rotors **1** were strongly correlated with $\Delta G^{\ddagger}_{exp}$ (R^2 = 0.97), as indicated by the blue triangles in Figure 4b, which is consistent with TS stabilizing secondary electrostatic interactions. As the charge on C2 becomes more positive, the barrier decreases, following the expected trend for an attractive electrostatic interaction with an electronegative oxygen. Interestingly, a correlation was also observed between the natural charge of C1 and the rotational barrier (Figure 4b, black circles). However, this was an inverse correlation. As the C1 charge became more positive, the barrier increased, which is contrary to the expected trend for an attractive electrostatic interaction with an electronegative oxygen.

Comparisons of the natural charges in the transition states of the rotor R-groups and analogous S_N2 electrophiles (Figure 4c) confirmed that the rotors effectively model secondary electrostatic interactions. Not only was there an excellent correlation between the natural charges on C2 of the rotors and S_N2 electrophiles (R^2 = 0.996), but their absolute values were also very similar. For example, the natural charges in rotor **1** R-groups ranged from -0.542 e (R = CH_2CH_3) to 0.328 e (R = CH_2CN). The natural charges in the S_N2 electrophiles spanned a similar range, from -0.610 e ($ClCH_2CH_3$) to 0.315 e ($ClCH_2CN$). This confirms that the through-space secondary electrostatic interactions in the rotor model systems will be comparable to those in the S_N2 reaction.

While significant orbital interactions between the imide oxygen and C1 are unlikely, they cannot be entirely ruled out. The imide oxygen lone pairs could form non-covalent tetrel bonds or other n → σ* interactions with C1.[26,27] The orbital component of these non-covalent interactions could participate in a conjugation effect with C2. To assess the magnitude of these effects, we performed secondary perturbation NBO analyses of the intermolecular TS energies. These analyses revealed weak orbital interactions (<3 kcal/mol), which are significantly weaker than the 30–50 kcal/mol orbital component of a fully formed C–O bond of an S_N2 reaction (see SI section 11). Interestingly, these interactions were with the hydrogens on C1 rather than the carbon. Overall, the NBO analyses confirmed that orbital effects involving C1 are minor and were unlikely to significantly influence the observed trends.

The molecular rotor approach provided an alternative approach to determine whether non-covalent interactions involving C1 could explain the observed trends. To investigate this, we designed rotors **2**, which have different first atoms. In rotors **2**, the C1 CH_2-groups of rotors **1** were replaced with O, S, $N(CH_3)$, $CH(CH_3)$, and C=O groups. The rotors were constructed in pairs, featuring either sp^3 methyl or sp^2 phenyl carbon at C2, to test whether the secondary sp^2 effect could be observed in different environments. The through-space secondary interactions should be independent of the nature of the first atom. Therefore, the faster rates observed for systems with sp^2 versus sp^3 C2 carbons should be observable when the first atom is not an sp^3 methylene carbon. This is difficult to test in S_N2 reactions where the sp^3 C1 carbon is involved in the key bond formation and breaking processes. In contrast, in the rotors, C1 does not form a bond, making it possible to test this aspect of the secondary interaction-based hypothesis.

The faster rate of rotation for the benzyl versus aliphatic rotors was observed for all six rotor pairs (Figure 4d), matching the trend observed for rotor **1** (**1**(CH_2CH_3) versus **1**(CH_2Ph) and providing additional support for the secondary electrostatic hypothesis. For example, **2**(OCH_3) and **2**(OPh) had barriers of 20.2 and 18.2 kcal/mol, which equates to 2.0 kcal/mol lower barrier for **2**(OPh) which has an sp^2 second carbon. Similar trends were observed for other sp^3/sp^2 pairs: 0.7 kcal/mol for **2**(SCH_3) and **2**(SPh), 1.8 kcal/mol for **2**($N(CH_3)_2$) and **2**($N(CH_3)$Ph), and 1.0 kcal/mol for **2**($COCH_3$) and **2**(COPh). Overall, rotors with sp^2 C2 carbons consistently had barriers that were, on average, 1 kcal/mol lower than rotors with sp^3 C2 carbons. This consistent trend, regardless of the first atom, provides further support for the secondary electrostatic hypothesis.

In conclusion, this study provides valuable insights into the mechanistic understanding of S_N2 reactions and the role of secondary electrostatic effects in shaping their outcomes. Specifically, it provides strong experimental evidence supporting the secondary electrostatic interaction hypothesis in S_N2 reactions. Using a series of molecular rotors designed to isolate

and measure through-space interactions, we demonstrated and measured the kinetic effects of secondary electrostatic interactions. Rotors with sp^2 and sp C2 carbons had 0.5 to 2.0 kcal/mol lower rotational barriers compared to rotors with sp^3 C2 carbons. These trends align with the enhanced reactivity of benzylic and allylic electrophiles in S_N2 reactions, indicating that both processes are likely governed by similar principles. Computational analysis confirmed the presence of stabilizing electrostatic interactions between C2 and the C=O oxygen in the rotor transition state. Additionally, these effects persisted across different electrophilic atom environments, reinforcing secondary electrostatic interactions as a key factor in S_N2 reactivity differences. This work establishes molecular rotors as an effective tool for probing the influence of non-covalent and through-space interaction in reaction transition states. We are currently applying this methodology to study and predict the reactivity of other reactions, including Michael additions and S_NAr reactions, to further explore the role of weak non-covalent forces in chemical reactivity and selectivity.

Supporting Information

Crystal structure for **1**(CH_2CN) is provided.[28] The authors have cited additional references within the Supporting Information.[29–33]

Acknowledgments

Funding for this work was provided by the National Science Foundation grants CHE 2003889 and 2304777.

Keywords: nucleophilic substitution; reaction mechanism; molecular devices; electrostatic interactions; supramolecular

References

[1] C. Ingold, *Structure and Mechanism in Organic Chemistry*, Bell, London, **1969**.
[2] J. Xie, W. L. Hase, *Science* **2016**, *352*, 32–33.
[3] J. Xie, R. Otto, J. Mikosch, J. Zhang, R. Wester, W. L. Hase, *Acc. Chem. Res.* **2014**, *47*, 2960–2969.
[4] T. A. Hamlin, M. Swart, F. M. Bickelhaupt, *ChemPhysChem* **2018**, *19*, 1315–1330.
[5] I. Szabó, G. Czakó, *Nat. Commun.* **2015**, *6*, 5972.
[6] D. O'Hagan, J. W. Schmidberger, *Nat. Prod. Rep.* **2010**, *27*, 900.
[7] R. H. DeWolfe, W. G. Young, *Chem. Rev.* **1956**, *56*, 753–901.
[8] L. F. Hatch, V. Chiola, *J. Am. Chem. Soc.* **1951**, *73*, 360–362.
[9] J. F. King, G. T. Y. Tsang, M. M. Abdel-Malik, N. C. Payne, *J. Am. Chem. Soc.* **1985**, *107*, 3224–3232.
[10] A. Streitwieser, *Chem. Rev.* **1956**, *56*, 571–752.
[11] I. Erden, S. Gronert, J. R. Keeffe, J. Ma, N. Ocal, C. Gärtner, L. L. Soukup, *J. Org. Chem.* **2014**, *79*, 6410–6418.
[12] R. D. Bach, B. A. Coddens, G. J. Wolber, *J. Org. Chem.* **1986**, *51*, 1030–1033.
[13] C.-H. Wu, B. Galabov, J. I.-C. Wu, S. Ilieva, P. Von R. Schleyer, W. D. Allen, *J. Am. Chem. Soc.* **2014**, *136*, 3118–3126.
[14] B. Galabov, G. Koleva, H. F. Schaefer, W. D. Allen, *Chem. – Eur. J.* **2018**, *24*, 11637–11648.
[15] B. Galabov, V. Nikolova, J. J. Wilke, H. F. Schaefer, W. D. Allen, *J. Am. Chem. Soc.* **2008**, *130*, 9887–9896.
[16] R. E. Rawlings, A. K. McKerlie, D. J. Bates, Y. Mo, J. M. Karty, *Eur. J. Org. Chem.* **2012**, *2012*, 5991–6004.
[17] P. R. Rablen, B. D. McLarney, B. J. Karlow, J. E. Schneider, *J. Org. Chem.* **2014**, *79*, 867–879.
[18] A. Streitwieser, *Solvolytic Displacement Reactions*, McGraw-Hill, **1962**.
[19] A. M. Schoevaars, W. Kruizinga, R. W. J. Zijlstra, N. Veldman, A. L. Spek, B. L. Feringa, *J. Org. Chem.* **1997**, *62*, 4943–4948.
[20] A. Ciogli, S. Vivek Kumar, M. Mancinelli, A. Mazzanti, S. Perumal, C. Severi, C. Villani, *Org. Biomol. Chem.* **2016**, *14*, 11137–11147.
[21] F. G. Bordwell, W. T. Brannen, *J. Am. Chem. Soc.* **1964**, *86*, 4645–4650.
[22] E. C. Vik, P. Li, P. J. Pellechia, K. D. Shimizu, *J. Am. Chem. Soc.* **2019**, *141*, 16579–16583.
[23] B. Lin, H. Liu, I. Karki, E. C. Vik, M. D. Smith, P. J. Pellechia, K. D. Shimizu, *Angew. Chem. Int. Ed.* **2023**, e202304960.
[24] B. Lin, H. Liu, H. M. Scott, I. Karki, E. C. Vik, D. O. Madukwe, P. J. Pellechia, K. D. Shimizu, *Chem. – Eur. J.* **2024**, e202402011.
[25] L. Lunazzi, M. Mancinelli, A. Mazzanti, S. Lepri, R. Ruzziconi, M. Schlosser, *Org. Biomol. Chem.* **2012**, *10*, 1847.
[26] S. Scheiner, *Phys. Chem. Chem. Phys.* **2021**, *23*, 5702–5717.
[27] A. Bauzá, T. J. Mooibroek, A. Frontera, *ChemPhysChem* **2015**, *16*, 2496–2517.
[28] *CCDC Deposition Number 2409542*.
[29] S. H. Alelaiwi, J. R. McKee, *ACS Omega* **2021**, *6*, 6009–6016.
[30] R. M. Parrish, L. A. Burns, D. G. A. Smith, A. C. Simmonett, A. E. DePrince, E. G. Hohenstein, U. Bozkaya, A. Yu. Sokolov, R. Di Remigio, R. M. Richard, J. F. Gonthier, A. M. James, H. R. McAlexander, A. Kumar, M. Saitow, X. Wang, B. P. Pritchard, P. Verma, H. F. Schaefer, K. Patkowski, R. A. King, E. F. Valeev, F. A. Evangelista, J. M. Turney, T. D. Crawford, C. D. Sherrill, *J. Chem. Theory Comput.* **2017**, *13*, 3185–3197.
[31] G. M. Sheldrick, *Acta Crystallogr. Sect. C Struct. Chem.* **2015**, *71*, 3–8.
[32] G. M. Sheldrick, *Acta Crystallogr. Sect. Found. Adv.* **2015**, *71*, 3–8.
[33] O. V. Dolomanov, L. J. Bourhis, R. J. Gildea, J. A. K. Howard, H. Puschmann, *J. Appl. Crystallogr.* **2009**, *42*, 339–341.

Entry for the Table of Contents

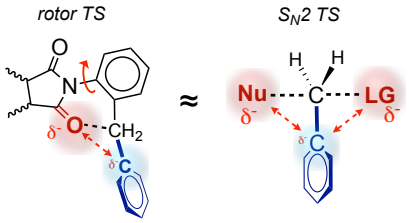

This study experimentally tests the role of secondary electrostatic interactions in S_N2 reactions using molecular rotors. Lower rotational barriers for sp^2/sp carbons align with faster S_N2 rates, isolating these effects from conjugation. The results reveal electrostatic interactions as a key factor, confirmed across diverse atoms like O, S, and N.